https://doi.org/10.3311/PPci.41308

Periodica Polytechnica Civil Engineering

An Efficient Kriging Surrogate Model for Developing Seismic Fragility Curves of Low-rise Steel Structures Considering Epistemic Uncertainties

Fooad Karimi Ghaleh Jough[1*], Sasan Babaei[1]

[1] Department of Civil Engineering, Faculty of Engineering, Final International University, Eğitim Kurumları Limited Beşparmaklar Avenue, No:6, 99370, via Mersin 10, Kyrenia, North Cyprus, Türkiye
[*] Corresponding author, e-mail: fooad.karimi@final.edu.tr

Received: 17 June 2025, Accepted: 14 January 2026, Published online: 19 February 2026

Abstract

Seismic fragility curves are essential for assessing structural performance under earthquake loading; however, their development requires addressing both aleatory and epistemic uncertainties, which can be computationally intensive. This study introduces an efficient Kriging-based surrogate modeling framework for deriving collapse fragility curves of steel moment-resisting frames while explicitly incorporating uncertainties in key hysteretic parameters. Incremental Dynamic Analysis (IDA) is conducted on a 5-story steel frame using 22 far-field ground motions and 125 structural parameter scenarios, reflecting probabilistic variability in plastic rotation capacity, post-capping rotation, and cyclic deterioration. The Kriging surrogate is calibrated using maximum likelihood estimation, enabling accurate interpolation of nonlinear structural response behavior. Validation results demonstrate a prediction accuracy of $R^2 = 0.92$, outperforming the conventional response surface method ($R^2 = 0.88$). Additionally, the Kriging model reduces mean collapse capacity prediction error to 0.5%, compared to 24% in the response surface approach, while maintaining significantly lower computational cost. The proposed methodology provides a computationally efficient and uncertainty-aware framework for collapse fragility curve development, supporting performance-based seismic design and risk assessment.

Keywords

fragility curve, Kriging model, uncertainties, response surface method, steel moment frame

1 Introduction

Structural collapse during earthquakes remains a critical concern, motivating deeper investigation into the factors contributing to such failures. Among these, lateral instability or sideway collapse triggered by seismic ground motions has received significant attention in recent studies [1–3]. Efforts to address this issue have focused on improving evaluation methods to better understand and mitigate this form of structural damage. These approaches emphasize incorporating uncertainties related to seismic loads and structural behavior, resulting in more reliable predictions of collapse capacity and the development of probabilistic collapse fragility curves. Such curves, which relate ground motion intensity to the probability of structural failure, are a cornerstone of consequence based earthquake engineering, playing a vital role in seismic loss estimation for both collapse and non-collapse states [4]. Uncertainties in fragility analyses arise from two primary sources: aleatory uncertainties due to the inherent randomness of seismic records and modeling uncertainties stemming from limitations in analytical modeling [5, 6]. While traditional methods, such as Monte Carlo simulations with Response Surface Method (RSM), offer robust solutions, their high computational demands make them less practical for large-scale applications. To address these limitations, response surface methods have been proposed, though their reliance on fixed functional forms introduces constraints [7]. In recent years, artificial neural networks (ANNs) have proven to be highly effective, offering the flexibility to approximate complex functions without relying on predefined assumptions. This capability makes them especially suitable for probabilistic collapse analyses. Previous studies have demonstrated the effectiveness of ANNs in deriving fragility curves for various structural limit states, integrating randomness in material properties, geometry, and seismic inputs [8]. To tackle complex engineering challenges, ANNs provide an effective and versatile approach for modeling [9]. One notable application of

Cite this article as: Karimi Ghaleh Jough, F., Babaei, S. "An Efficient Kriging Surrogate Model for Developing Seismic Fragility Curves of Low-rise Steel Structures Considering Epistemic Uncertainties", Periodica Polytechnica Civil Engineering, 2026. https://doi.org/10.3311/PPci.41308

ANNs is their use in function approximation and system prediction. These networks are particularly effective when nonlinear relationships exist between system inputs and outputs. The performance of an ANN largely depends on its architectural design and training process. Evolutionary algorithms, recognized as population-based random search methods, have proven effective in optimizing ANN design and training, making them a popular choice among researchers. However, in intricate networks, overtraining can occur, which diminishes the network's ability to generalize. To enhance predictive accuracy, especially for solving complex problems with limited data samples, hybrid ANNs have emerged as a valuable approach [10]. ANNs were utilized to construct fragility and incremental dynamic analyses (IDA) curves for assessing various structural damage states. Records parameters and properties of acceleration were employed as inputs and outputs for the ANN model, respectively [11]. The advanced fuzzy algorithm was applied to derive the failure probability curve for steel moment frames (SMF), incorporating the values of the trilinear Ibarra model as modeling uncertainties. The results showed that this approach offered improved computational efficiency compared to traditional probabilistic methods [12]. Furthermore, an integration of Deep learning models and RSM with the Monte Carlo-based RSM approach was used to drive collapse vulnerability profiles for steel moment frames (SMF). It was found that the Monte Carlo-based ANN simulation provided more accurate estimations of the average values and dispersion measures of the vulnerability profiles compared to the RSM-based approach [13]. Fragility curves were developed using an advanced fuzzy methodology, which proved advantageous in terms of precision and computational speed [14]. Recent studies have also examined fragility-based vulnerability assessment of bridge and tall building systems, and explored surrogate and reduced-order modeling to improve the computational efficiency of fragility curve derivation [15–18]. A novel approach integrating logistic functions and neural networks was developed for software reliability analysis. The method utilized PSO algorithms with forward propagation architecture, demonstrating enhanced predictive accuracy in reliability growth modeling [19]. A study of seismic risk in moment frames was conducted using the nonlinear Ibarra-Krawinkler modified anchor model, specifically focusing on near-fault earthquake effects [20]. This study builds on these advancements by applying an ANN-based approach to develop collapse fragility curves, explicitly accounting for both aleatory and epistemic uncertainties. The methodology involves training a three-layer Kriging-enhanced surrogate model using data from IDA of a three-story SMF exposed to variable modeling parameters and seismic excitations. The target output, spectral acceleration at collapse $Sa_{(\text{collapse})}$, is used to generate fragility curves through Monte Carlo simulations based on Kriging-Enhanced Surrogate Modeling. By comparing the proposed method with response surface method, this work highlights the efficiency and accuracy of Kriging-based models in capturing epistemic uncertainty effects on collapse fragility curves. The assessment of structural collapse performance has become a pivotal research focus in earthquake engineering due to the substantial economic, environmental, and human losses caused by structural failures during seismic events. The intricacies involved in structural collapse, coupled with significant uncertainties in modeling and simulating collapse responses, have driven the need for more robust and computationally efficient methodologies for evaluating collapse performance and predicting associated risks. These efforts are indispensable for modern seismic design, which aims to enhance safety and optimize structural performance under extreme seismic loading conditions. A systematic approach to evaluate global structural collapse was established based on the correlation between Seismic intensity measures (*IM*) and structural response parameters [21]. They referred global failure as the structural system's inability to sustain gravity loads under seismic influences. In the final step, the intensity measure (*IM*) increases until the response parameter becomes unstable, as indicated by a flat *IM*–EDP curve (slope = 0). The highest relative intensity at this point is termed the collapse failure. Numerous tests have been conducted on reinforced concrete columns to update and fine-tune the values of the tri-linear Ibarra model. Through statistical analyses and multivariable regression, they developed empirical relations for these parameters [22]. Structural response Measure, such as median and standard deviation (SD) of collapse capacity, are affected by a wide array of factors, including the inherent uncertainties in structural properties and the variability of seismic ground motions. To address these complexities, structural component parameters are often modeled probabilistically. This study employs the Ibarra-Krawinkler moment–rotation parameters to represent modeling uncertainties, enabling a comprehensive evaluation of collapse behavior across diverse scenarios. Furthermore, correlations between parameters within individual components and across multiple structural components are considered to ensure a realistic depiction of structural variability. To overcome the

computational challenges associated with such high-dimensional uncertainty modeling, this research introduces an innovative Kriging-Enhanced Hybrid (KEH) modeling framework for seismic performance prediction. Unlike conventional surrogate or response surface methods that rely on predefined functional relationships, the proposed KEH framework integrates Kriging's probabilistic interpolation with adaptive hybrid learning, allowing the model to self-optimize parameter selection and capture complex nonlinear interactions even under limited training data. This methodological advancement significantly reduces the number of simulations required for reliable collapse prediction while maintaining high predictive accuracy. The proposed approach represents a substantial improvement over existing ANN- or RSM-based fragility curve models, as it unifies statistical rigor and machine learning flexibility in a single probabilistic platform. Specifically, the KEH method enables accurate and efficient prediction of collapse fragility curves, risk, and reliability while explicitly quantifying both aleatory and epistemic uncertainties. By minimizing computational cost and enhancing uncertainty representation, this study establishes a new direction in surrogate-based seismic fragility modeling. A key focus of this analysis is the derivation of collapse fragility curves, which quantify the likelihood of structural failure under varying levels of seismic intensity. These curves play a crucial role in seismic risk assessment and loss estimation, providing a probabilistic framework for evaluating structural performance across different damage states. This study accounts for both aleatory uncertainties (record-to-record variability in seismic ground motions) and epistemic uncertainties (arising from incomplete knowledge of structural behavior). Incremental Dynamic Analysis (IDA) is utilized to compute the spectral acceleration corresponding to the sidesway damage state for various structural scenarios, serving as input for training the KEH model [23]. The proposed KEH approach demonstrates its efficacy in accurately predicting structural collapse responses even with a limited number of uncertainty samples. The results are compared against those obtained from the response surface method, showcasing the advantages of the hybrid method in terms of computational efficiency and predictive accuracy. In conclusion, this study presents a novel hybrid Kriging-based surrogate modeling framework that not only improves accuracy and efficiency but also advances the state-of-the-art in collapse fragility assessment by providing a unified, uncertainty-aware, and data-efficient predictive tool for performance-based seismic design.

2 Prediction function

2.1 Monte Carlo method

Monte Carlo Simulation (MCS) is a widely used technique for reliability analysis in steel structures, effectively addressing uncertainties in material properties, applied loads, and geometric configurations. The methodology involves defining a limit state function $G(X) = R(X) - S(X)$, where $R(X)$ represents the resistance or capacity of the structure, and $S(X)$ represents the applied loads or stress effects. Structural failure occurs when $G(X) \leq 0$, delineating the failure domain [24].

In practice, MCS generates a large number of random samples for the input variables based on their probabilistic distributions, such as normal or log-normal distributions. The limit state function $G(X)$ is evaluated for each sample, and the failure probability P_f is estimated as [24]:

$$P_f = \frac{N_f}{N} \tag{1}$$

where N_f is the count of failure cases and N is the total number of simulations. To simplify, an indicator function $I(G(X))$ can be used, where $I(G(X)) = 1$ if $G(X) \leq 0$, and $I(G(X)) = 0$ otherwise. In this representation [24]:

$$P_f = \frac{1}{N}\sum_{i=1}^{N} I\left(G\left(X_i\right)\right). \tag{2}$$

Despite its robustness in dealing with complex and nonlinear systems, MCS can be computationally intensive, particularly when estimating low probabilities of failure [24].

To enhance computational efficiency, the Monte Carlo method can be integrated with advanced surrogate modeling techniques. One promising approach is to combine MCS with Kriging-based surrogate modeling. Kriging, a statistical interpolation method, predicts the output of expensive simulations with high accuracy by modeling the spatial correlation between data points. By employing Kriging, we can significantly reduce the number of required simulations while maintaining accuracy in reliability analysis.

Additionally, combining this framework with Artificial Neural Networks (ANNs) or response surface methods allows for efficient prediction and optimization in structural reliability assessments. By leveraging the strengths of Kriging as a surrogate model in conjunction with Monte Carlo simulations, this hybrid approach provides a powerful tool for improving computational efficiency and accuracy in analyzing the seismic performance and reliability of steel structures.

RSM is a mathematical method widely used in engineering and reliability analysis to approximate the relationship

between input variables (factors) and a response parameter (output). The core idea is to create a simplified model often a polynomial approximation of the complex and computationally expensive function representing the structural performance or failure. In reliability analysis, the response parameter typically represents the structural capacity or safety margin, denoted as $Y = G(X)$, where $G(X)$ is the limit state function, and $X = \{x_1, x_2, .. x_n\}$ are the random variables influencing the structural behavior. The RSM approximates this function using a polynomial regression model, commonly up to the second degree, as follows [24]:

$$\hat{Y} = \beta_0 + \sum_{i=1}^{n} \beta_i \chi_i + \sum_{i=1}^{n} \sum_{j=1}^{n} \beta_{ij} \chi_i \chi_j \quad (3)$$

where:

- β_0 is the intercept term,
- β_i are the coefficients of the linear terms,
- β_{ij} are the coefficients of the interaction terms between the variables x_i and x_j,
- x_i and x_j are the input variables (e.g., material properties, loads, geometric parameters).

2.1.1 Surrogate modeling: foundations and principles

The primary objective of reliability estimation is to determine the probability of failure, a task achieved through mathematical integration [9]. The probability of failure P_f is calculated as the probability that the limit state function $G(X)$ is less than zero, expressed as an integral:

$$P_f = P[G(X) \le 0] = \int ... \int_{G(X) \le 0} f_x (X_1, X_2, ..., X_n) \mathrm{d}X_1 \, \mathrm{d}X_2 \cdots \mathrm{d}X_n \quad (4)$$

where $f_x(.)$ denotes the joint probability density function (PDF), X represents the random variables, $G(.)$ is the limit state function, $G(.) \le 0$ signifies failure events, and n corresponds to the number of random variables [25].

The Kriging metamodel constitutes an interpolation technique grounded in statistical theory, encompassing both a parametric linear regression model and a nonparametric stochastic process. The initial design of experiments is denoted as [25]:

$$X = \{x_1, x_2, \ ..., \ x_{n0}\} \quad (5)$$

where each $x_i \ \epsilon \ R^n$ represents an experiment. Correspondingly:

$$G = \{G(x_1), G(x_2), \ ..., \ G(x_{n0})\} \quad (6)$$

captures the responses. The Kriging model establishes an approximate relationship [25]:

$$\hat{G}(x) = F(x, \beta) + z(x) = f^T(x)\beta + z(x) \quad (7)$$

statistical characteristics are defined as [25, 26]:

$$E(z(x)) = 0 \quad (8)$$

$$Var(z(x)) = \sigma_z^2 \quad (9)$$

$$Cov(z(x_i), z(x_j)) = \sigma_z^2 R(x_i, x_j, \theta). \quad (10)$$

The Gaussian correlation model is [25, 26]:

$$R(x_i, x_j) = \exp\left(-\sum_{k=1}^{n} \theta_k (x_i^k - x_j^k)^2 \right), \theta_k > 0 \cdot \quad (11)$$

The estimates for μ and σ^2 are [25]:

$$\hat{\mu} = (F^T R^{-1} F)^{-1} F^T R^{-1} G \quad (12)$$

$$\sigma_z^2 = \frac{1}{N_0} (G - F\mu)^T R^{-1} (G - F\mu). \quad (13)$$

Also, the correlation parameter θ is determined through maximum likelihood estimation [25]:

$$\hat{\theta} = \arg\min_\theta (N_S \ln \hat{\sigma}_G^2 + \ln|R|). \quad (14)$$

For any chosen θ, an interpolation model is established, and the optimal Kriging model is derived by optimizing θ. At an unknown point X, the Best Linear Unbiased Predictor of the response $\hat{G}(x)$ follows a Gaussian distribution, given by [25]:

$$\hat{G}(x) \sim \mathcal{N}(\hat{\mu_G}(x), \hat{\sigma}_G(x)), \quad (15)$$

where [25]:

$$\hat{\mu}_G(x) = \beta + r^T(x) R^{-1} (G - \beta F) \quad (16)$$

$$\hat{\sigma}_G^2(x) = \sigma_G^2(x) \left(1 + u^T(x) (F^T R^{-1} F)^{-1} u^T(x) - r^T(x) R^{-1} r(x)\right). \quad (17)$$

Here, $r^T(x)$ represents the correlation vector between X and the initial design of experiments points, and $u(x)$ is calculated as [25]:

$$u(x) = F^T R^{-1} r(x)) - 1. \quad (18)$$

The choice to employ a Kriging model for our application stems from several key advantages that align with the specific characteristics and demands of the reliability assessment problem. Kriging models offer a unique capability in capturing spatial variability within the data, a crucial aspect of our system where spatial correlation plays a significant role. By leveraging geostatistical methods, Kriging provides a robust framework for interpolating between observed data points, ensuring a more accurate representation of the system's behavior. One notable strength of Kriging lies in its ability to rigorously account for the spatial distribution of data, a feature grounded in geostatistics. This is particularly

beneficial in scenarios where spatial correlation information is essential for reliable predictions. The geostatistical foundation of Kriging contributes to its effectiveness in regions where data points may be scarce or unavailable, allowing for a more comprehensive understanding of the system. Furthermore, Kriging inherently provides estimates of prediction uncertainty. This is a critical aspect in reliability assessments, enabling not only accurate predictions but also a quantification of the confidence associated with those predictions [26]. The uncertainty quantification feature enhances the reliability of the model, especially when dealing with complex systems where uncertainties are inherent. Adaptive sampling strategies, crucial for improving model accuracy and efficiency, are seamlessly facilitated by Kriging. This adaptability ensures that new samples are strategically acquired in regions with high uncertainty, optimizing the use of computational resources. Particularly in cases with a high-dimensional input space, Kriging demonstrates efficiency, requiring fewer samples compared to some alternative surrogate modeling techniques.

3 Structural instability metrics and damage probability curves

IDA is a widely used technique to evaluate the vulnerability of structures under varying intensities in seismic zones. This method requires selecting appropriate parameters that represent the Ground Motion Parameter (*IM*) and the Structural Response Parameter (*DM*). When subjected to various ground motion, a structure exhibits varying behaviors, as illustrated in Fig. 1. One such behavior is static instability, which occurs when the structure softens under increasing seismic demands, leading to large drifts and eventual collapse. A minor increase in *IM* results in a disproportionate growth in deformation, culminating in the *IM-DM* curve flattening out as the *DM* approach extremely high values. Some structures also exhibit a combination of hardening and softening behaviors, where the slope or "stiffness" of the *IM-DM* curve alternates between decreasing and increasing with higher *IM* levels. This indicates an acceleration and deceleration in the rate of accumulation of *DM*. In certain cases, deceleration is so pronounced that *DM* momentarily stabilizes or even reduces, leading to a non-monotonic *IM-DM* relationship. This phenomenon, while initially counterintuitive, has been documented in previous research. Under specific seismic conditions, systems demonstrating significant responses at moderate intensity levels may exhibit reduced responses at higher intensities due to hardening effects.

The progression of seismic intensity amplifies cycles with weak initial responses, altering structural characteristics for subsequent cycles. This leads to changes such as period elongation or extreme hardening, which can momentarily restore structural stability. However, at certain intensity levels, these changes push the system toward global instability, where numerical analysis diverges, and *DM* becomes theoretically infinite. IDA has been endorsed by FEMA-350 for analyzing structural collapse capacities. Identifying collapse through numerical methods is crucial for determining a structure's capacity [27]. Two primary approaches are commonly used: tracking the "softening" of the *IM-DM* curve and identifying instances of numerical instability. In the softening approach, the curve flattens as structural reserves for resisting lateral displacements diminish, causing minor increments in IM to trigger disproportionate responses. FEMA-350 defines flattening as occurring when the *IM-DM* slope decreases to less than 20% of the original tangent. While simple, this term may not accurately reflect experimental observations for large *DM*s, requiring careful engineering judgment. The second approach, numerical instability, occurs when the solution algorithm cannot converge due to the degradation of structural stiffness, often resulting from extensive plastic deformations or hinge formation. This loss of redundancy in the structural model, particularly in cases with negligible material hardening, can make the solution of equilibrium equations infeasible, even for small force increments. Nonconvergence might also stem from algorithmic or modeling limitations unrelated to collapse. Advanced dynamic algorithms are therefore essential to accurately capture abrupt changes in structural response caused by nonlinearities. Overall, while each criterion for determining structural collapse has its limitations, they provide valuable insights into the behavior and capacity of structures under seismic excitations.

The integration of engineering judgment and empirical validation remains critical to refining these approaches. Although the engineering demand parameters (EDPs) defined in Table 4–10 of FEMA 350 for low-rise steel buildings were adopted in this study to identify different damage states, the collapse threshold was determined using the IM-based (intensity-measure-based) criterion [27]. In this approach, collapse corresponds to the last converged point on the IDA curve before numerical instability occurs. This point represents the seismic intensity level (IM collapse) at which the structure can no longer maintain equilibrium due to severe degradation of stiffness and strength, leading to non-convergence in the dynamic analysis. This approach more realistically accounts for the remaining capacity of the structure, particularly the effects of material hardening, compared to the more conservative EDP-based method.

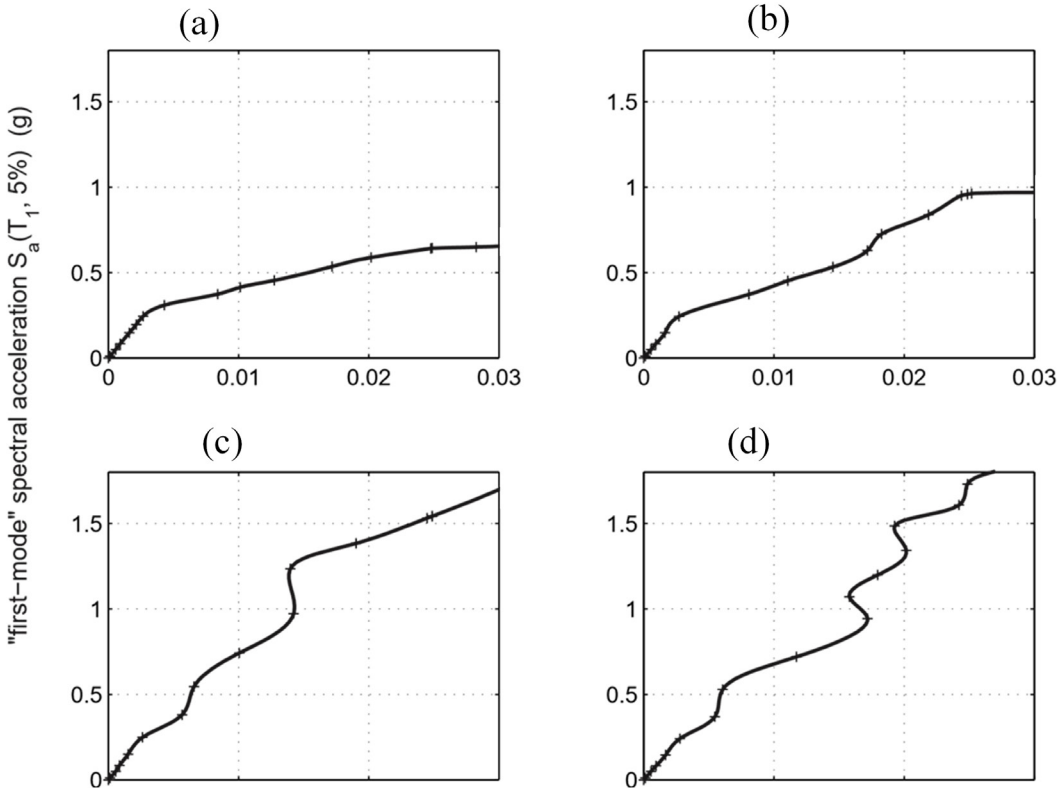

Fig. 1 Different collapse possibility in IDA curves: (a) a softening case, (b) a bit of hardening, (c) severe hardening, and (d) weaving behavior [23]

For each IDA curve, there exists a specific seismic intensity associated with structural collapse, referred to as *IM* collapse. Additionally, the collection of these points across multiple IDA curves can be used to generate collapse fragility curves, which represent the probability of structural failure. The likelihood of structural collapse is mathematically expressed as shown in Eq. (19) [23]:

$$P_{F|X=x} = \phi\left(\frac{\ln x - \eta_x}{\xi_X}\right) \tag{19}$$

where η_X and ξ_X show the median and SD of collapse fragility curve respectively, based on *X*. median and SD are derived using Eqs. (20) and (21) [23]:

$$\eta_x = \frac{1}{N}\sum_{k=1}^{N} \ln x_k \tag{20}$$

$$\xi_x = \sqrt{\frac{\sum_{k=1}^{N}\left(\ln x_k - \eta_x\right)^2}{N-1}} \tag{21}$$

where x_k represents the *X* value of set *k*, and *N* is the total set of earthquake scenarios.

4 Performance base earthquake engineering criteria

The core methodology of Performance-Based Earthquake Assessment focuses on computing the mean annual frequency (λ) of exceedance for specific limit states. This computation utilizes an advanced form of the risk integral, validated by the Pacific Earthquake Engineering Research Center, where the base equation is expressed as [28, 29]:

$$\lambda(X) = \iint\left[\phi(X|DM)\Psi(DM|IM)|\eta(IM)|\right] \tag{22}$$

As shown in Eq. (22), $\lambda(X)$, $\phi(X)$, and $\psi(DM)$ represent the annual frequency function, response distribution, and complementary distribution function respectively, with *IM* denoting the intensity measure and $\eta(IM)$ characterizing the seismic hazard function. For practical implementation, Eq. (22) can be reformulated as [30]:

$$\lambda_X = \int_{IM=0}^{\infty} F_X(IM)|\eta(IM) \tag{23}$$

where the response function is defined by

$$f_X(IM) = \int_{x=0}^{\infty}\left|\frac{\partial\Psi(X|IM)}{\partial X}\right|\left|\frac{\partial IM}{\partial X}\right|dX\,. \tag{24}$$

The formulation in Eqs. (23) and (24) enables direct integration over the intensity measure domain, providing a more straightforward approach to capacity evaluation. When the response parameter *X* is predetermined, Eq. (23) can be further simplified to [30]:

$$\lambda_X = \int_0^{\infty} F_X(IM)|\eta(IM)| \tag{25}$$

where $F_X(IM)$ represents the capacity distribution function as defined in Eq. (24). The probability of failure can be efficiently estimated using simulation methods through [31]:

$$P_f = \frac{1}{N}\sum_{i=1}^{N} I\left(IM_i < IM_{cap}\right). \quad (26)$$

As demonstrated in Eq. (26), $I(\cdot)$ serves as an indicator function and N represents the total number of simulations. This approach, combining Eqs. (22)–(26), provides a robust method for evaluating structural performance under seismic loading, particularly when dealing with complex structural systems where closed-form solutions may not be readily available. The methodology maintains consistency with established earthquake engineering practices while offering flexibility in implementation for various structural configurations and performance criteria [23].

5 Modeling and sensitive analysis

5.1 Structural configuration and design parameters

The seismic performance of moment-resisting steel frames has gained significant attention due to their enhanced lateral resistance capabilities. This research investigates the 5-story steel moment resisting frame structure, designed with moderate ductility for residential occupancy in Tehran, which is located in a high seismic hazard zone with a design base acceleration of 0.35 g according to Standard 2800 [32]. These structures were designed in accordance with the National Building Code [33] requirements and Standard 2800 [32]. As illustrated in Fig. 2, the structures were initially developed using three-dimensional modeling before being simplified to a two-dimensional frame analysis incorporating *P*-Delta effects through a leaning column approach. The study focuses on a perimeter frame configuration where the peripheral frames, except for the end columns and their connecting beams, are modeled with pinned connections [34].

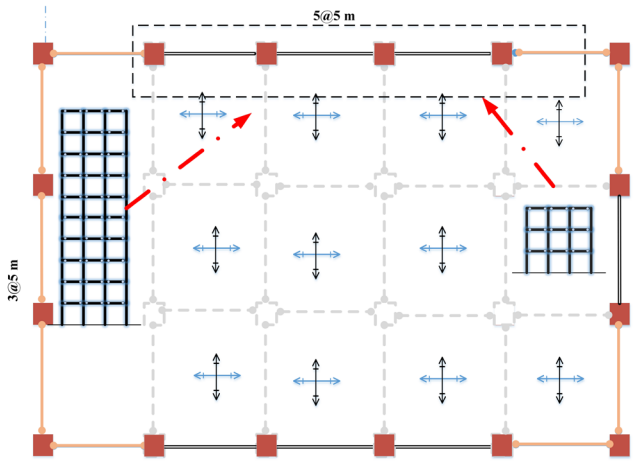

Fig. 2 Plan and elevation of the study structure

To accurately capture second-order effects and gravity load influences, a leaning column was incorporated into the analytical model. This column, connected to the main frame with rigid links at each floor level, carries the tributary gravity loads from the interior frames that are not directly modeled in the two-dimensional analysis.

The leaning column was modeled with pinned connections at each floor and designed to be axially rigid but with minimal flexural stiffness. This ensured proper transmission of *P*–Delta effects without contributing to lateral resistance. In the gravity load analysis, dead loads from both interior frames and peripheral elements were appropriately distributed to the structural system through the leaning column, considering the high seismic demands of the region. The structural configuration maintains a consistent story height of 3 m throughout the building, with an enhanced first story height of 4 m to accommodate architectural requirements. The bay width is uniformly set at 5 m across all frames. The building is situated on soil type II according to local regulations, which significantly influences the seismic response characteristics of both structures. The structural system utilizes ST37 grade steel throughout its components. In compliance with Standard 2800 and considering Tehran's high seismicity, the design incorporates stringent drift limitations: an allowable relative lateral displacement of 0.025 for the 5-story building [32]. The design methodology prioritizes economic efficiency while maintaining strict adherence to strength and serviceability requirements particularly critical for high seismic zones. Following the tenth edition of the National Building Code, the design implements strength reduction factors of 0.9 for flexural members and 0.75 for compression elements.

5.2 Rotational parameters of concentrated plastic hinge model

For structural modeling and analysis, OpenSEES (Open System for Earthquake Engineering Simulation) software was utilized, which offers capabilities for both linear and nonlinear analyses while accounting for hysteretic behavior. In this framework, the selected hysteretic model must be capable of modeling factors affecting structural behavior, including elastic behavior, inelastic (plastic) behavior of members, joint behavior, and various degradation characteristics due to deterioration, stiffness degradation, strength reduction, and local buckling [35]. The concentrated plasticity model (plastic hinge) has been employed in this approach. Each beam-column element consists of an elastic beam-column member with two zero-length rotational plastic springs with degrading behavior at both ends. In the elastic

behavioral state, since the beam is modeled elastically, the two springs should theoretically be modeled as rigid. However, due to finite element considerations and the singularity of the stiffness matrix caused by rigid members ($K \rightarrow \infty$), the model becomes numerically unstable. To prevent this issue, springs must be modeled as non-rigid, where $K_{spring} < \infty$. In this case, the springs participate in deformation and result in larger-than-actual deformations. To overcome this limitation, analytical equations derived from linear behavioral conditions have been utilized. In the elastic behavioral state of the beam, the elastic stiffness (K_e) and spring stiffness (K_s) are derived from rigid stiffness, expressed as $K_{total} = (1/K_e + 1/K_s)^{-1}$, which corresponds to the behavior of an elastic member and rigid stiffness for springs. In the nonlinear behavioral state, the springs with degrading behavior due to deterioration provide highly accurate deformation results. The rotational spring characteristics are determined based on tri-linear member curves and experimental studies [36]. The modified Ibarra-Krawinkler deterioration model has been implemented in this research (Fig. 3 [37]). Through extensive testing of I-shaped beams and BOX-shaped columns, Krawinkler modified the Ibarra-Krawinkler model to present deterioration models that enabled more accurate prediction of element behavior up to failure levels. These new deterioration curves can predict post-failure strength loss, residual strength (F_{res}), and ultimate deformation capacity (θ_u).

In Fig. 3, M_y is the effective yield moment, M_c is the elastic modulus multiplied by yield strength, M_p (κM_y) represents the post-yield moment capacity, θ_y is the yield rotation, θ_p is the plastic rotation capacity, θ_c is the capping rotation capacity, θ_u is the ultimate rotation capacity, $\theta_{cap,pl}$ is the post-capping rotation capacity, and θ_{pc} is the post-capping rotation capacity after the cap point. The capacity for energy component is defined by Eq. (27).

$$E_t = \Lambda M_y \tag{27}$$

In Eq (27), Λ represents the rate of cyclic deterioration, which is evaluated through the calibration of experimental results. This parameter is considered a critical modeling factor in this study. Previous research has shown that θ_P, θ_{pc}, and Λ significantly influence the collapse performance of structures. Therefore, in this study, these three parameters are selected as the primary modeling parameters, including their inherent epistemic uncertainties. As shown in Fig. 4 [38], joint2D elements were used to model connections that significantly affect the linear and nonlinear story drifts of the steel frame. The panel zone exhibits very high stiffness due to the use of box sections for columns, characterized by $K_{panel} = GA_v/d_b$, where G is the shear modulus, A_v is the shear area of panel zone, and d_b is the beam depth [35]. The cyclic behavior modeling incorporates three key uncertain parameters: plastic rotation capacity (θ_p), post-capping rotation capacity (θ_{pc}), and the cyclic deterioration parameter (Λ). Experimental calibration studies have demonstrated that these parameters follow log-normal probability distributions. Table 1 presents the statistical characteristics of these modeling variables, including their median values, dispersions, and correlation coefficients.

5.3 IDA and fragility curve

The selection of ground motion records for IDA was conducted following FEMA-P695 protocols [39]. The *IM* was selected as the 5% Reduced spectral acceleration at the primary period ($S_a(T_1)$), in accordance with FEMA P695 (2009) guidelines. For the structural response assessment, the maximum inter-story drift ratio (θ_{max}) was adopted as the

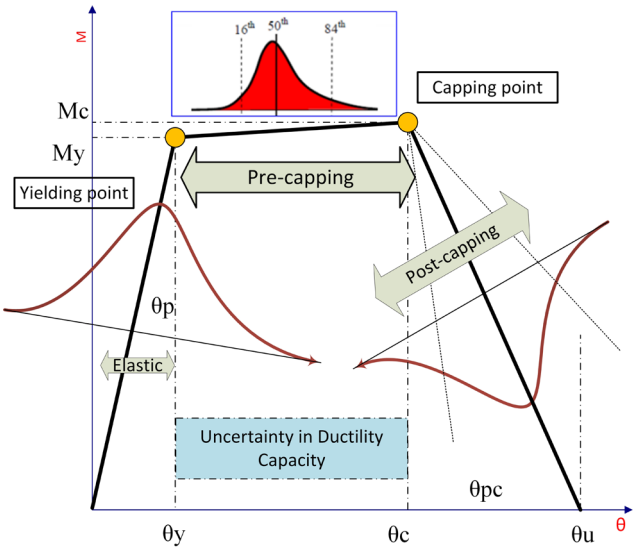

Fig. 3 The simplified backbone curve and hysteresis loop are based on the modified IMK model [37]

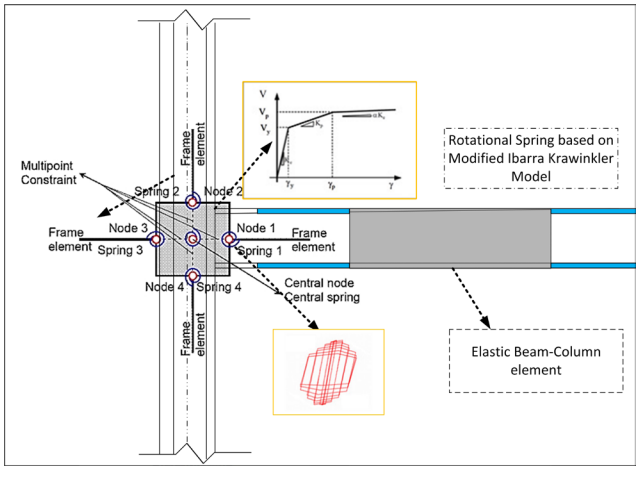

Fig. 4 Joint2D element architecture for connection modeling dissipation of the structural [38]

Table 1 Statistical parameters of component deterioration model based on experimental calibration [37]

Model parameters and correlation coefficients								
Plastic Rotation		Post-capping		Deterioration		Correlation		
Median θ_p	σ_{θ_p}	Median θ_{pc}	$\sigma_{\theta_{pc}}$	Median Λ	σ_Λ	$\rho_{\theta_p,\theta_{pc}}$	$\rho_{\theta_p,\Lambda}$	$\rho_{\theta_{pc},\Lambda}$
0.025	0.43	0.16	0.41	1.00	0.43	0.69	0.44	0.67

primary demand parameter, accounting for both story-to-story variations and temporal evolution throughout the seismic excitation. The IDA implementation utilized the Hunt&Fill algorithm, as proposed by Vamvatsikos and Cornell, which provides an efficient approach for conducting the incremental analyses [23]. The ground motion records used for IDA in this study consist of 22 pairs of records (44 components) selected from the FEMA-P695 far-field record set. These records are from earthquakes where the site-to-source distance exceeds 10 km.

The initial phase of the proposed methodology focuses on establishing functional relationships for the mean and standard deviation of fragility curve parameters with respect to the structural modeling parameters. This framework has been implemented using Monte Carlo simulation techniques integrated with response surface methodology. The procedure requires selecting a discrete set of modeling parameter values to determine the statistical characteristics (mean and standard deviation) of the fragility curve through incremental dynamic analysis. The response surface, fitted to the analytical results, incorporates both the mean and standard deviation functions of the fragility parameters, utilizing complete second-order polynomial functions for the mathematical representation. To determine the approximate values of the fragility curves, different values of modeling parameters have been selected to define the mean and standard deviation of the frame fragility curves. For each modeling variable, the mean value, mean minus two standard deviations, and mean plus two standard deviations have been combined. Considering 3 modeling variables, a total of 125 cases have been analyzed through incremental dynamic analysis. Fig. 5 shows the schematic representation of the selected modeling parameters and illustrates the total number of considered cases.

The methodology employs Incremental Dynamic Analysis (IDA) for each realization of input variables to determine the collapse spectral acceleration (SA_{collapse}) for individual ground motion records, which then serves as target data for the proposed neural network framework, utilizing 40 × 125 vectors for training and testing purposes (representing 125 parameter combinations and 22 ground motion records), with representative IDA curves and fragility curve for 5 story structure illustrated in Fig. 6. This diagram represents a state of the structure where only aleatory uncertainty is considered, without accounting for epistemic uncertainty.

6 Epistemic uncertainty

6.1 Response surface methodology and statistical analysis

In the response surface methodology, we aim to replace the response values with a function of input variables (θ_p, θ_{pc}, and Λ) to obtain the best fit $f(X)$ that yields the minimum deviation from actual values (minimum error). When the number of input variable samples is limited, accurate prediction of the response function becomes challenging. In this research, to determine the required number of simulations, we utilized the central composite design method for the incremental dynamic analysis, where a total of 125 simulations were required at one central factorial point at the sixteenth level. The proposed model for the response function is based on uncertainties using a quadratic model. The *p*-value approach was implemented to assess the significance of terms in the quadratic model (Eq. (3)), where terms

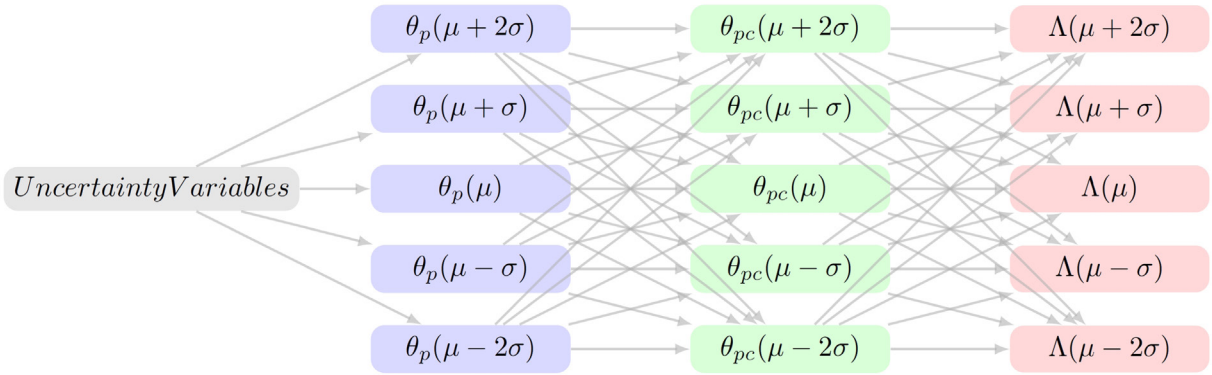

Fig. 5 Hierarchical representation of uncertainty variables and their relationships in structural parameters

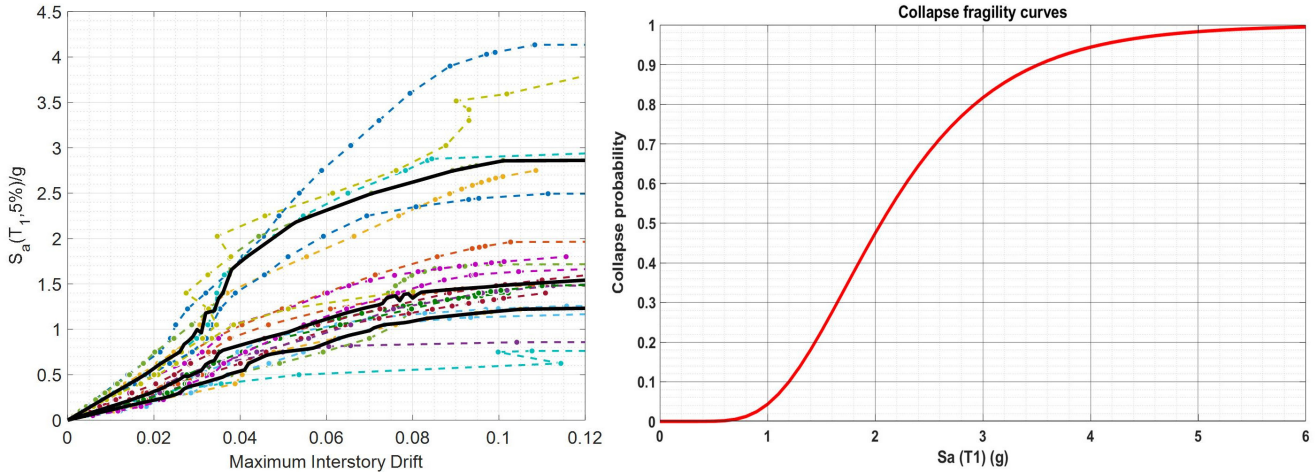

Fig. 6 IDA and fragility curve of 5-story structure

with larger *p*-values indicate less significance in the model. Specifically, *p*-value < 0.05 indicates significant terms, while *p*-value > 0.1 indicates non-significant terms, and consequently, all terms with *p*-value > 0.1 were removed from the model. Equations (28) and (29) present the mean collapse capacity function and standard deviation function in terms of independent normal variables (θ_p, θ_{pc}, and Λ) [24]. The corresponding coefficients are provided in Table 2. Figs. 7 and 8 show the correlation diagram between target data and output data, along with correlation coefficient values and prediction accuracy assessment. For such simulations, statistical measures including mean square error, root mean square error, error histogram, mean error values, and standard deviation of errors for both collapse capacity mean and standard deviation were evaluated. Errors in the estimation of means and standard deviations of collapse fragility curves are compared with the Kriging model in the next section.

$$\mu_{\ln(S_{A_c})} = \beta_0 + \sum_{i=1}^{N}\beta_i x_i + \sum_{i<j}^{N}\beta_{ij}x_i x_j + \sum_{i=1}^{N}\beta_i x_i^2 = \beta_0 + \beta_1\theta_p + \beta_2\theta_{pc} + \beta_3\Lambda + \beta_4\theta_p\theta_{pc} + \beta_5\theta_p\Lambda + \beta_6\theta_{pc}\Lambda + \beta_7\theta_p^2 + \beta_8\theta_{pc}^2 + \beta_9\Lambda^2 \quad (28)$$

$$\sigma_{\ln(S_{A_c})} = \beta'_0 + \sum_{i=1}^{N}\beta'_i x_i + \sum_{i<j}^{N}\beta'_{ij}x_i x_j + \sum_{i=1}^{N}\beta'_i x_i^2 = \beta'_0 + \beta'_1\theta_p + \beta'_2\theta_{pc} + \beta'_3\Lambda + \beta'_4\theta_p\theta_{pc} + \beta'_5\theta_p\Lambda + \beta'_6\theta_{pc}\Lambda + \beta'_7\theta_p^2 + \beta'_8\theta_{pc}^2 + \beta'_9\Lambda^2 \quad (29)$$

Table 2 Response surface coefficients

	Mean Function ($\mu_{Ln}(SAc)$)
β_0–β_9	{−0.24, −37.23, 4.02, 0.93, −29.35, 2.89, 0.572, 830.984, −6.378, −0.297} Standard Deviation ($\sigma_{Ln(SAc)}$)
β'_0–β'_9	{−0.57, 74.321, −0.636, 0.13, 15.028, −1.56, 0.216, −1458.47, 0.475, −0.118}

6.2 Kriging model methodology to predict fragility curve

The effectiveness of the Kriging model is validated using statistical metrics that compare predictions against actual observed values. Two key metrics are employed: the mean squared prediction error (MSPE) and the coefficient of determination (R^2), defined as [25]:

$$\text{MSPE} = \frac{1}{N}\sum_{i=1}^{N}\left(\hat{G}(x_i) - G(x_i)\right)^2 \quad (30)$$

$$R^2 = 1 - \frac{\sum_{i=1}^{N}\left(\hat{G}(x_i) - G(x_i)\right)^2}{\sum_{i=1}^{N}\left(G(x_i) - \bar{G}\right)^2} \quad (31)$$

where $\hat{G}(x_i)$ represents the predicted value, $G(x_i)$ is the observed value, and $\bar{G}$ is the mean of observed values. A higher R^2 value indicates better model fit.

For predicting behavior at unknown points, the Best Linear Unbiased Predictor (BLUP) is utilized [26]:

$$\hat{G}(x) = \mu_{\hat{G}(x)} + r(x)^T R^{-1}\left(G - F\beta\right) \quad (32)$$

where $\mu_{\hat{G}(x)}$ is the BLUP mean, $r(x)$ is the correlation vector between the unknown point x and observed points, R and G represent the correlation matrix and observed responses vector respectively, and β and F are regression coefficients and design matrix.

The predicted values for mean ($\hat{\mu}$) and standard deviation ($\hat{\sigma}$) are calculated as [26]:

$$\hat{\mu} = f_{1T}\left(\theta_p, \theta_{pc}, \Lambda\right)\beta_1 + z_1\left(\theta_p, \theta_{pc}, \Lambda\right) \quad (33)$$

$$\hat{\sigma} = f_{2T}\left(\theta_p, \theta_{pc}, \Lambda\right)\beta_2 + z_2\left(\theta_p, \theta_{pc}, \Lambda\right). \quad (34)$$

Using Radial Basis Functions (RBFs), the basis function is expressed as

$$f\left(\theta_p, \theta_{pc}, \Lambda\right) = \sum_{j=1}\beta_j\phi_j\left(\theta_p, \theta_{pc}, \Lambda\right) + z\left(\theta_p, \theta_{pc}, \Lambda\right) \quad (35)$$

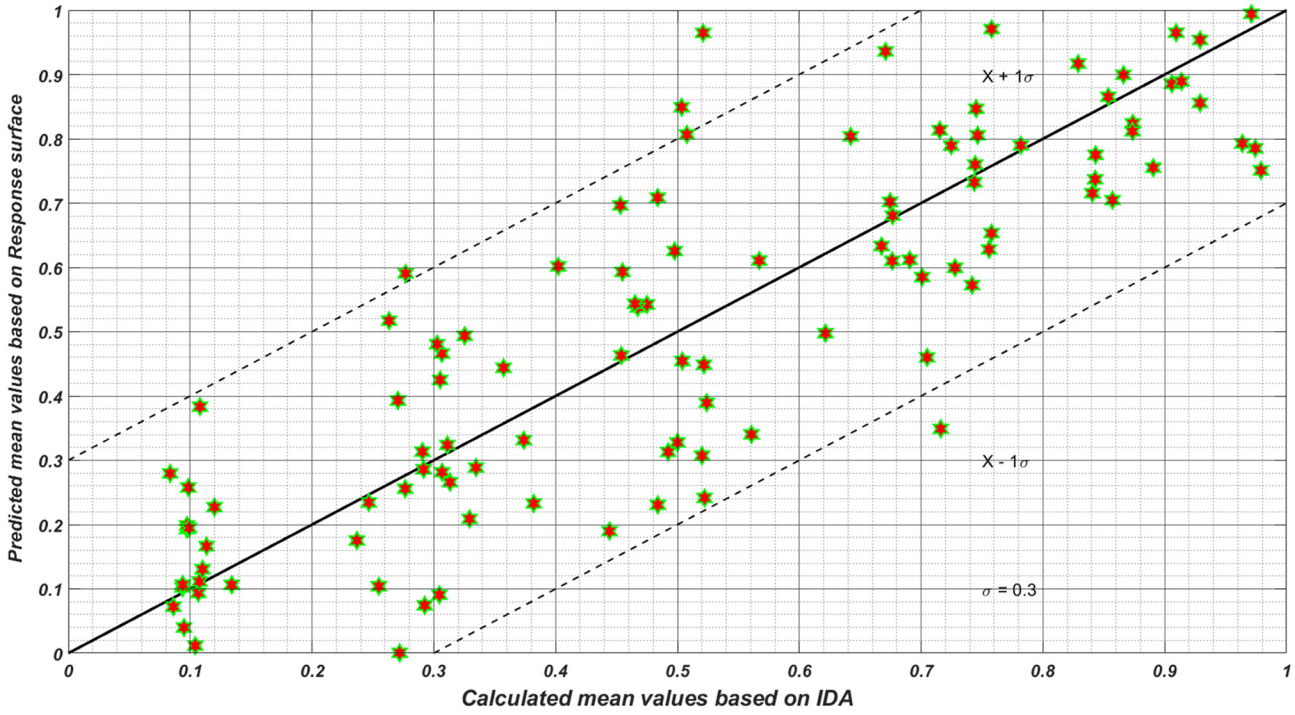

Fig. 7 The figure compares the IDA-based collapse capacity (horizontal axis) with the predicted mean collapse capacity using Eq. (28) (vertical axis). Each point represents one case, and the 45° diagonal line represents the ideal scenario with perfect prediction accuracy.

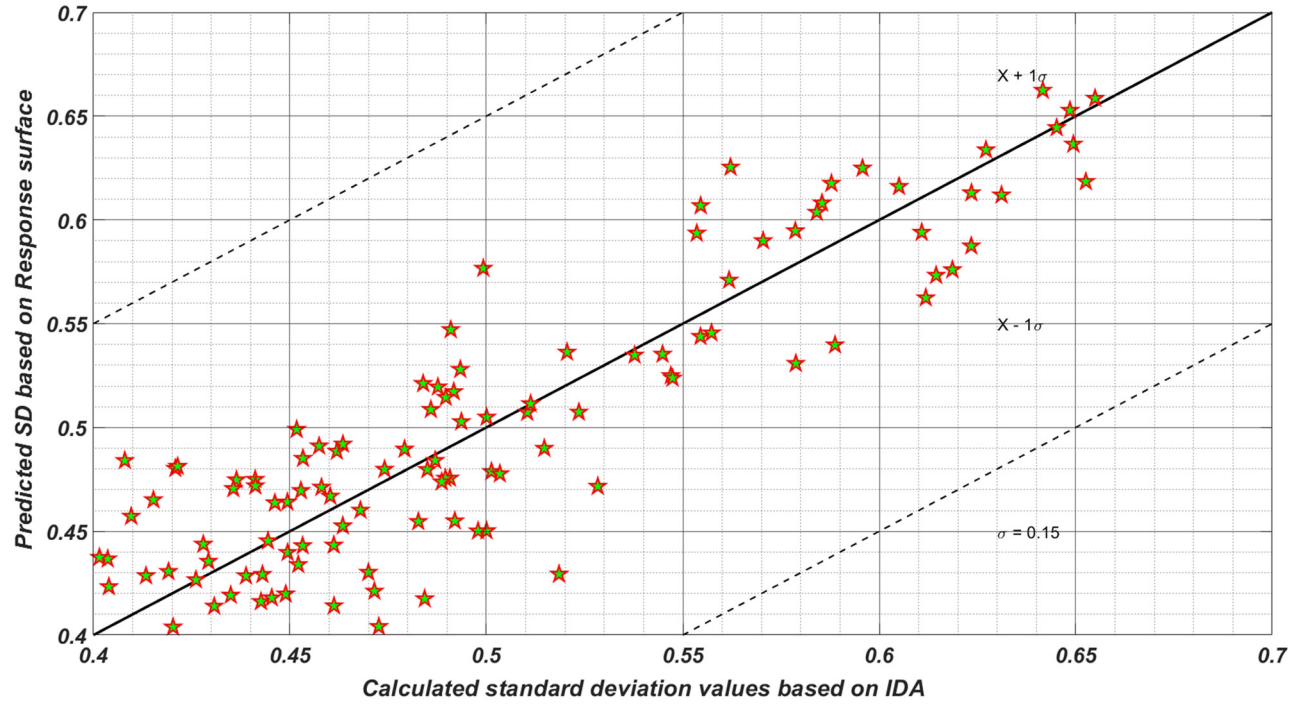

Fig. 8 The figure compares the IDA-based collapse capacity (horizontal axis) with the predicted standard deviation using Eq. (29) (vertical axis). Points located on the 45° line indicate perfect agreement, while deviations reflect prediction error.

$$\phi_j\left(\theta_p,\theta_{pc},\Lambda\right)= \exp\left(-\frac{\left\|\theta_p-M_{j1}\right\|^2+\left\|\theta_{pc}-M_{j2}\right\|^2+\left\|\Lambda-M_{j3}\right\|^2}{2S_j^2}\right)\cdot \tag{36}$$

Finally, the weighted averaging approach is applied:

$$\mu_{\text{weighted}}=\frac{\sum_{i=1}^{N}\mu_i\omega_i}{\sum_{i=1}^{N}\omega_i} \tag{37}$$

$$\sigma_{\text{weighted}} = \frac{\sum_{i=1}^{N} \sigma_i \omega_i}{\sum_{i=1}^{N} \omega_i} \tag{38}$$

where N is the number of predictions and ω_i represents the weight assigned to the i^{th} prediction.

In this section, the performance of the Kriging method in predicting the relative displacement of the aforementioned frames was investigated. For 90 randomly selected samples, the predicted relative mean and SD values of these frames were compared with the actual outputs. The coefficient values R^2 for the 5-story frames was calculated as 0.92. These values demonstrate the capability of the Kriging surrogate model in predicting the response of smart material-equipped structural models. In other words, it is evident that there exists a strong linear correlation between the actual relative Sa_c values of the mentioned frames and the predicted response based on the Kriging method, showing minimal error in predicting the structural responses. To verify the accuracy and precision of the Kriging surrogate models, according to Eqs. (39)–(41), the Mean Square Error (MSE), Mean Absolute Error (MAE), and correlation coefficient (R^2) indices were calculated and compared. The Mean Square Error and Mean Absolute Error always have a positive value; the closer these values are to zero, the lower the error. The results of the statistical parameters obtained from the Kriging surrogate models are presented in Table 3.

$$\text{MSE} = \frac{\sum_{i=1}^{N} \left(R_{\text{Pre}} - R_{\text{IDA}} \right)^2}{N} \tag{39}$$

$$\text{MAE} = \frac{\sum_{i=1}^{N} \left| R_{\text{Pre}} - R_{\text{IDA}} \right|}{N} \tag{40}$$

$$R^2 = \frac{\left[\sum_{i=1}^{N} \left(R_{\text{Pr}e} - \bar{R}_{\text{Pr}e} \right) \left(R_{\text{IDA}} - \bar{R}_{\text{IDA}} \right) \right]^2}{\sum_{i=1}^{N} \left(R_{\text{Pr}e} - \bar{R}_{\text{Pr}e} \right)^2 \sum_{i=1}^{N} \left(R_{\text{IDA}} - \bar{R}_{\text{IDA}} \right)^2} \tag{41}$$

Where R_{Pre} and R_{IDA} are the predicted and IDA-based responses, respectively, and $\bar{R}_{\text{Pre}}$ and $\bar{R}_{\text{IDA}}$ represent their mean values [24].

Table 3 Statistical parameters results obtained from Kriging surrogate models and Response surface method

Statistical Parameters	Kriging surrogate models	Response surface method
MSE	23.3	55
MAE	2.5	4.1
R^2	0.92	0.88

To further evaluate the prediction performance, the percentage error was calculated to quantify the largest deviation between the predicted structural responses and those obtained from Incremental Dynamic Analysis (IDA). This metric is defined as

$$\text{Error}\% = \left(\frac{\left| R_{\text{Pre}(i)} - R_{\text{IDA}(i)} \right|}{R_{\text{IDA}(i)}} \right) \times 100 \tag{42}$$

where $R_{\text{Pre}(i)}$ and $R_{\text{IDA}(i)}$ represent the predicted response and the IDA-based response for sample i, respectively. Based on the testing dataset, the Kriging model demonstrated substantially lower prediction errors in estimating collapse capacity compared to the Response Surface Method (RSM), particularly in regions exhibiting strong nonlinear behavior close to structural collapse. Table 4 summarizes the percentage errors obtained for the mean and standard deviation predictions of collapse capacity.

The relatively high errors associated with the RSM are attributed to its limited capability in representing highly nonlinear structural responses near collapse, where stiffness degradation and instability become dominant. In contrast, the Kriging model maintains accuracy by effectively learning localized correlation patterns and propagating associated uncertainties. These results further highlight the superiority of the Kriging-enhanced surrogate modeling approach for collapse prediction and fragility assessment.

To develop the collapse fragility curves, two distinct approaches were implemented. In the first approach, the Kriging surrogate models was employed to estimate mean and SD of $\text{SA}_{\text{collapse}}$ for 10,000 simulated input variables. The collapse fragility curve was then obtained by fitting a probability distribution to these mean and SD values.

For the second approach, response surface methodology was utilized to estimate the statistical parameters (mean and standard deviation) of the collapse fragility curve. This estimation was based on 10,000 simulations of the modeling variables. The effectiveness of the proposed methodology was validated through comparison with alternative methods, as illustrated in Fig. 9. Additionally, Fig. 9 presents the collapse fragility curve where modeling uncertainties are excluded (i.e., using mean values for all modeling parameters).

Table 4 Prediction error of collapse fragility statistics (mean and standard deviation) for Kriging and response surface approaches

Predicted parameter	Response Surface method (%)	Kriging model (%)
Mean values	24	0.5
Standard deviation values	6	3.7

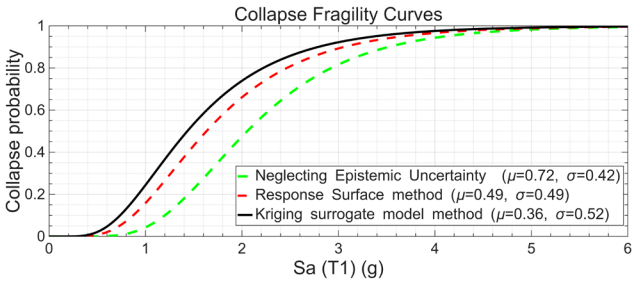

Fig. 9 Comparison of the effects of including versus neglecting epistemic uncertainty on the collapse fragility curve

This dual-approach methodology enables a comprehensive assessment of structural collapse probability while accounting for various sources of uncertainty in the modeling process. The response surface methodology exhibits significant limitations when incorporating epistemic uncertainties, primarily due to its reliance on predefined functional forms for characterizing the statistical parameters (mean and standard deviation) of fragility curves. This constraint becomes particularly problematic in collapse limit state analysis, where structures exhibit highly nonlinear behavior. The fixed mathematical framework of response surfaces may not adequately capture the complex relationships and interactions that emerge during structural collapse.

Conversely, the Kriging surrogate approach offers a more versatile framework for predicting mean and SD. The Kriging architecture, employs a two-component predictor consisting of a polynomial regression function representing the global trend and a Gaussian correlation function characterizing local deviations, where the correlation parameters are optimized through maximum likelihood estimation to enhance prediction accuracy in interpolating between sampled points. This flexibility enables more accurate representation of structural response under extreme loading conditions.

The resulting collapse fragility curves are derived by fitting lognormal distribution functions to the SA_{collapse} values, providing a more robust characterization of structural vulnerability that inherently accounts for the system's nonlinear behavior.

By comparing the error generated in predicting the collapse responses at 16%, 50%, and 84% levels using the response surface method and Kriging method, it can be concluded that both methods achieve errors less than 10%. In predicting the mean collapse capacity, mean drift ratio, and mean annual frequency of collapse, these methods demonstrate nearly identical performance and possess desirable capability in estimating structural collapse responses.

For a high number of simulations, the Kriging method predicts structural responses in less time compared to the response surface method. This is because for each simulation, the generated values for uncertainties must be substituted in Eqs. (28) and (29) to obtain the structural responses, which is somewhat time-consuming given the high number of terms in Eqs. (28) and (29). However, by neglecting the interaction effects between uncertainties in the above relationships, one can generate equations with fewer terms for a large number of simulations, although this leads to reduced accuracy and increased error in response prediction using the response surface method. Nevertheless, the analysis time and response prediction in the response surface method remains negligible compared to incremental dynamic analysis.

As mentioned in previous sections, the annual limit state frequency (λ) is obtained by computing the area under the curve of the product of the fragility function and the absolute increment of spectral acceleration hazard function through numerical integration of the aforementioned quantities.

For better comparison, the results of basic and uncertain models for sidesway collapse that is near to Collapse Prevention and Immediate Occupancy (IO) limit state are presented in Table 5 and depited in Fig. 10. it can be observed that the impact of capacity uncertainty on seismic demand estimation in the (IO) limit state is negligible. In contrast, comparing the limit state frequency of basic and uncertain models at the Collapse Prevention (CP) limit state reveals that capacity uncertainty has significantly increased the annual probability of failure. This increase stems from the differences between two parameters - the mean and standard deviation - of the uncertain model compared to the basic model, indicating that capacity uncertainty has led to a reduce in mean and increase in standard deviation relative to the basic model. It is worth noting that even small changes in these values led to a significant increase in the annual limit-state frequency. This aspect has received limited attention in previous studies, where the effects of capacity uncertainty on structural performance were not thoroughly investigated.

7 Conclusions

In this study, an innovative Kriging-Enhanced Hybrid (KEH) surrogate modeling framework was proposed to efficiently predict the seismic collapse fragility curves of steel moment-resisting frames while incorporating both aleatory and epistemic uncertainties. The developed approach effectively addresses the computational challenges associated with conventional response surface and Monte Carlo-based methods. Application of the proposed model to a five-story steel frame demonstrated remarkable predictive performance and stability. The Kriging

Table 5 Annual limit state frequency for Base and uncertain model parameters

Limit State	Base Model		Kriging model		Response surface	
	IO	CP	IO	CP	IO	CP
Annual Frequency	3.825e-4	2.025e-5	3.62e-4	2.99e-5	3.72e-4	3.03e-5

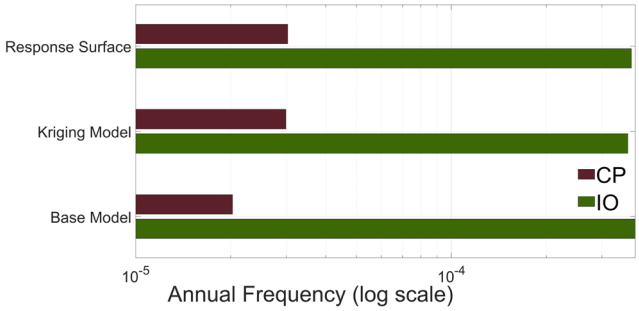

Fig. 10 Annual limit state frequencies (in log scale) for IO and CP across different modeling approaches (Base Model, Kriging Model, and Response Surface)

model achieved an R^2 of 0.92, compared with 0.88 for the traditional Response Surface Method (RSM). The mean collapse capacity prediction error decreased from 24% (RSM) to only 0.5% (KEH), while the standard deviation error was reduced from 6% to 3.7%. Similarly, the mean absolute error (MAE) dropped from 4.1 to 2.5, and the mean squared error (MSE) from 55 to 23.3, confirming the superior precision of the Kriging-based framework. In addition to its precision, the KEH model required over 50% fewer simulations than traditional Incremental Dynamic Analysis (IDA), achieving comparable reliability in predicting collapse fragility curves. The framework efficiently captured the effects of modeling uncertainties, resulting in smoother and more realistic fragility distributions across multiple damage states. Overall, the proposed KEH framework establishes a robust, uncertainty-aware, and computationally efficient methodology for seismic fragility curve development. By integrating probabilistic interpolation with adaptive hybrid learning, it advances the state of surrogate-based modeling in performance-based earthquake engineering and provides a practical foundation for future studies on fragility analysis, seismic reliability, and risk-informed structural design.

References

[1] Karimi G. J., F., Şensoy, S. "Steel Moment-Resisting Frame Reliability via the Interval Analysis by FCM-PSO Approach Considering Various Uncertainties", Journal of Earthquake Engineering, 24(1), pp. 109–128, 2020. https://doi.org/10.1080/13632469.2017.1401564

[2] Hu, J. W., Shokrgozar, H. R., Golsefidi, E. S., Mansouri, I. "Effects of Brace Configuration and Structure Height on Seismic Performance of BRBFs Based on the Collapse Fragility Analysis", Periodica Polytechnica Civil Engineering, 64(4), pp. 1075–1086, 2020. https://doi.org/10.3311/PPci.13366

[3] Liu, C., Fang, D., Yan, Z. "Seismic Fragility Analysis of Base Isolated Structure Subjected to Near-fault Ground Motions", Periodica Polytechnica Civil Engineering, 65(3), pp. 768–783, 2021. https://doi.org/10.3311/PPci.15276

[4] Deierlein, G. G., Reinhorn, A. M., Willford, M. R. "Nonlinear Structural Analysis for Seismic Design: A Guide for Practicing Engineers", National Institute of Standards and Technology, Gaithersburg, MD, USA, Tech. Brief No. 4, 2010.

[5] Der Kiureghian, A., Ditlevsen, O. "Aleatory or epistemic? Does it matter?", Structural Safety, 31(2), pp. 105–112, 2009. https://doi.org/10.1016/j.strusafe.2008.06.020

[6] Zarif M. B. A., Pahlavan, H., Shafaie, J. "Probabilistic Seismic Performance Assessment of Tall RC Special Moment-Resisting Frame Buildings Equipped with Buckling-restrained Braces under Near-field Excitations", Periodica Polytechnica Civil Engineering, 68(2), pp. 524–542, 2024. https://doi.org/10.3311/PPci.20914

[7] Fardis, M. "Book Review: Seismic Reliability Analysis of Structures, by P. E. Pinto, R. Giannini and P. Franchin", Journal of Earthquake Engineering, 9(6), p. 943, 2005. https://doi.org/10.1142/S1363246905002353

[8] Jough, F. K. G. "Fuzzy Logic-Based Fragility Curve Development for Steel Moment-Resisting Frames Considering Uncertainties in Seismic Response", Journal of Earthquake and Tsunami, 18(5), 2450014, 2024. https://doi.org/10.1142/S1793431124500143

[9] Yao, X., Islam, M. M. "Evolving artificial neural network ensembles", IEEE Computational Intelligence Magazine, 3(1), pp. 31–42, 2008. https://doi.org/10.1109/MCI.2007.913386

[10] Karimi, G. J. F., Ghasemzadeh, B. "Uncertainty Interval Analysis of Steel Moment Frame by Development of 3D-Fragility Curves Towards Optimized Fuzzy Method", Arabian Journal for Science and Engineering, 49(4), pp. 4813–4830, 2024. https://doi.org/10.1007/s13369-023-08223-8

[11] Mitropoulou, C. C., Papadrakakis, M. "Developing fragility curves based on neural network IDA predictions", Engineering Structures, 33(12), pp. 3409–3421, 2011. https://doi.org/10.1016/j.engstruct.2011.07.005

[12] Zolfaghari, M. R., Beheshti Aval, S. B., Khojastehfar, E. "Uncertainty analysis using fuzzy randomness method towards development of fragility curves for moment-resisting steel structures", Scientia Iranica, 22(1), pp. 131–143, 2015.

[13] Karimi, G. J. F., Beheshti, A. S. B. "Uncertainty analysis through development of seismic fragility curve for an SMRF structure using an adaptive neuro-fuzzy inference system based on fuzzy C-means algorithm", Scientia Iranica, 25(6), pp. 2938–2953, 2018. https://doi.org/10.24200/sci.2017.4232

[14] Jough, F. K. G., Şensoy, S. "Prediction of seismic collapse risk of steel moment frame mid-rise structures by meta-heuristic algorithms", Earthquake Engineering and Engineering Vibration, 15(4), pp. 743–757, 2016. https://doi.org/10.1007/s11803-016-0362-9

[15] Naseri, A., Roshan, A. M., Pahlavan, H., Amiri, G. G. "Probabilistic seismic assessment of RC box-girder bridges retrofitted with FRP and steel jacketing", Coupled System Mechanics, 9(4), pp. 359–379, 2020. https://doi.org/10.12989/csm.2020.9.4.359

[16] Naseri, A., Mirza, R. A., Pahlavan, H., Ghodrati, A. G. "Numerical Analysis and Vulnerability Assessment of Horizontally Curved Multiframe RC Box-Girder and CFRP Retrofitting of Existing Bridges", ASCE-ASME Journal of Risk and Uncertainty in Engineering Systems, Part A: Civil Engineering, 8(3), 04022031, 2022. https://doi.org/10.1061/AJRUA6.0001236

[17] Xing, L., Gardoni, P., Zhou, Y. "Kriging metamodels for the dynamic response of high-rise buildings with outrigger systems and fragility estimates for seismic and wind loads", Resilient Cities and Structures, 1(1), pp. 110–122, 2022. https://doi.org/10.1016/j.rcns.2022.04.003

[18] Lee, S., Lee, J., Yoon, S., Lee, Y. J. "Efficient finite element reliability analysis employing sequentially-updated surrogate model for fragility curve derivation", Structures, 68, 107246, 2024. https://doi.org/10.1016/j.istruc.2024.107246

[19] Rani, P., Mahapatra, G. S. "A neuro-particle swarm optimization logistic model fitting algorithm for software reliability analysis", Proceedings of the Institution of Mechanical Engineers, Part O: Journal of Risk and Reliability, 233(6), pp. 958–971, 2019. https://doi.org/10.1177/1748006X19844784

[20] Beheshti-Aval, S. B., Khojastehfar, E., Noori, M., Zolfaghari, M. R. "A comprehensive collapse fragility assessment of moment resisting steel frames considering various sources of uncertainties", Canadian Journal of Civil Engineering, 43(2), pp. 118–131, 2016. https://doi.org/10.1139/cjce-2013-0491

[21] Ibarra, L. F., Medina, R. A., Krawinkler, H. "Hysteretic models that incorporate strength and stiffness deterioration", Earthquake Engineering &Structural Dynamics, 34(12), pp. 1489–1511, 2005. https://doi.org/10.1002/eqe.495

[22] Haselton, C. B., Liel, A. B., Lange, S. T., Deierlein, G. G. "Beam-Column Element Model Calibrated for Predicting Flexural Response Leading to Global Collapse of RC Frame Buildings", Pacific Earthquake Engineering Research Center, University of California, Berkeley, CA, USA, Rep. PEER 2007/03, 2007.

[23] Vamvatsikos, D., Cornell, C. A. "Applied Incremental Dynamic Analysis", Earthquake Spectra, 20(2), pp. 523–553, 2004. https://doi.org/10.1193/1.1737737

[24] Myers, R. H., Montgomery, D. C., Anderson-Cook, C. M. "Response Surface Methodology: Process and Product Optimization Using Designed Experiments", John Wiley & Sons, 2016. ISBN 978-1-118-91601-8

[25] Stein, M. L. "Interpolation of Spatial Data: Some Theory for Kriging", Springer, 1999. ISBN 978-0-387-98629-6 https://doi.org/10.1007/978-1-4612-1494-6

[26] Kaymaz, I. "Application of kriging method to structural reliability problems", Structural Safety, 27(2), pp. 133–151, 2005. https://doi.org/10.1016/j.strusafe.2004.09.001

[27] SAC Joint Venture "Recommended Seismic Design Criteria for New Steel Moment-Frame Buildings", Federal Emergency Management Agency, Washington, DC, USA, Rep. FEMA-350, 2000.

[28] Cornell, C. A. "Engineering seismic risk analysis", Bulletin of the Seismological Society of America, 58(5), pp. 1583–1606, 1968. https://doi.org/10.1785/BSSA0580051583

[29] Miranda, E., Aslani, H. "Probabilistic Response Assessment for Building-Specific Loss Estimation", Pacific Earthquake Engineering Research Center, College of Engineering, University of California, Berkeley, CA, USA, Rep. PEER 2003/03, 2003.

[30] Jalayer, F., Cornell, C. A. "A Technical Framework for Probability-Based Demand and Capacity Factor Design (DCFD) Seismic Formats", Pacific Earthquake Engineering Research Center, College of Engineering, University of California, Berkeley, CA, USA Rep. PEER 2003/08, 2003.

[31] Bazzurro, P., Cornell, C. A. "Disaggregation of Seismic Hazard", Bulletin of the Seismological Society of America, 89(2), pp. 501–520, 1999.

[32] BHRC "Standard No. 2800 Iranian code of practice for seismic resistant design of buildings", Building & Housing Research Center, Tehran, Iran, 2007.

[33] Ministry of Roads and Urban Development "Iranian National Building Regulations, Part 10: Design and Construction of Steel Structures", Office of National Building Regulations and Construction Control, Tehran, Iran, 2022. ISBN 978-600-113-414-2

[34] Baker, J., Cornell, C. A. "Vector-Valued Ground Motion Intensity Measures for Probabilistic Seismic Demand Analysis", Pacific Earthquake Engineering Research Center, University of California, Berkeley, CA, USA, Rep. PEER 2006-08, 2006.

[35] Ibarra, L. F., Krawinkler, H. "Global Collapse of Frame Structures under Seismic Excitations", John A. Blume Earthquake Engineering Center, Stanford, CA, USA, Report No. 152, 2005.

[36] Ellingwood, B. R., Kinali, K. "Quantifying and communicating uncertainty in seismic risk assessment", Structural Safety, 31(2), pp. 179–187, 2009. https://doi.org/10.1016/j.strusafe.2008.06.001

[37] Liel, A. B., Haselton, C. B., Deierlein, G. G., Baker, J. W. "Incorporating modeling uncertainties in the assessment of seismic collapse risk of buildings", Structural Safety, 31(2), pp. 197–211, 2009. https://doi.org/10.1016/j.strusafe.2008.06.002

[38] Foutch, D. A., Yun, S.-Y. "Modeling of steel moment frames for seismic loads", Journal of Constructional Steel Research, 58(5–8), pp. 529–564, 2002. https://doi.org/10.1016/S0143-974X(01)00078-5

[39] Federal Emergency Management Agency "Quantification of Building Seismic Performance Factors", Federal Emergency Management Agency, Washington, DC, USA, FEMA REP. P-695, 2009.